Vacuum 191 (2021) 110352

Contents lists available at ScienceDirect

Vacuum

journal homepage: www.elsevier.com/locate/vacuum

Angular distribution of ion beams energy and flux in a plasma focus device operated with argon gas

Mahsa Etminan, Farzin M. Aghamir *

Dept. of Physics, University of Tehran, Tehran, 14399-55961, Iran

ARTICLE INFO

Keywords:
Plasma focus device
Faraday cup
Ion beam energy
Ion beam flux

ABSTRACT

Energy and flux of ion beams in a Mather type (5 kJ) plasma focus device was investigated. The experiments were performed with argon as the chamber gas at the optimum pressure of 0.3 mbar and the charging voltage of 15 kV. Six identical Faraday cups located at angular positions 0, 15, 30, 45, 60 and 75° with respect to the anode axis were exploited to collect ion signals. The Faraday cups were mounted on a quadrant holder so that all Faraday cups have the same radial distance of 7 cm from the anode tip. In order to gain knowledge of target ions, when the plasma focus device is used for thin film deposition, three different targets of copper, graphite and tungsten were inserted on top of the anode tip. The ion signals registered by Faraday cups showed three main peaks relating to X-ray, argon gas and target ions, respectively. Plots of ion flux as a function of ions energy were obtained for argon gas and different targets separately. Energy spectra obtained from the Faraday cups revealed different anisotropies for argon gas and targets ions.

1. Introduction

Plasma focus (PF) device has the capability of being used effectively in material processing, ion implantation, semiconductor doping and thin film deposition. It is one of the prominent choices for energetic ions, relativistic electrons, fast neutrons and X-ray radiation. Emission of charged particles occurs as a result of plasma pinch and is affected by pinch dynamics. Recent studies show that in plasma focus device, after pinch formation, plasma plume has an asymmetric angular distribution of ions energy and density [1–3]. This anisotropy has been explained by the fact that ions are originated from different micro-sources which are created inside a dense pinched plasma column [3,4]. These micro-sources are not symmetrical with respect to the anode axis and they are characterized by different local parameters. Furthermore, the intensity of PF ion beam depends upon electrode geometry, capacitor bank energy, working gas type and pressure [5]. For each special condition, ions have different energy range and density at various angle and position with respect to anode tip. Ions flux angular distribution in plasma focus devices depends upon the working gas type. Mohanty et al. [3] showed that in a nitrogen filled PF device, ions flux along anode axis (0°) is less than that of the off axis and the maximum flux is obtained at 5°. Bhuyan et al. [1] using a set of five identical Faraday cups positioned at different angles 0°, 20°, 25°, 50° and 90° revealed that maximum neon ion beam flux is at 25° angular position. In yet another study, Bhuyan et al. [2] reported that among the dominant charge states of H^+, C^{4+} and C^{5+} obtained from methane operating gas, C^{4+} and C^{5+} ions flux maximizes at off axis (15°), while the maximum H^+ ion flux occurs at 0°. Similar results have been reported concerning the fact that maximum ion flux for H_2, deuterium and proton occurs along the anode axis [6–8]. Both the range and most probable energy of ion beam of nitrogen and methane gases are known to be irrespective of the angular position [2,3]. For neon ion beam, the most probable energy at 0° angular position has been larger than that of off axis [1].

Ions energy and density distribution are essential for understanding the physics behind production and acceleration of the PF device ions. Furthermore, it is vital to study and evaluate ions spatial energy and density distribution in order to optimize the use of plasma focus device in applications such as material processing and thin film deposition. The angular position has a crucial effect on these processes. In recent reports by Aghamir et al. [9,10], samples positioned at 60 and 75° with respect to anode axis experienced different depositional processes than those located near the axis. Their findings indicate that angular positions of 60 and 75° are more apt for forming crystal structures, whilst sample locations at 0 and 30° are more proper for ion implantation. Therefore, using PF as a material processing device involves knowledge of ions energy spectrum and flux at different angular position.

* Corresponding author.
E-mail address: aghamir@ut.ac.ir (F.M. Aghamir).

https://doi.org/10.1016/j.vacuum.2021.110352
Received 6 November 2020; Received in revised form 27 May 2021; Accepted 27 May 2021
Available online 2 June 2021

In the present study, thorough investigation of angular distribution of ions energy and flux is considered using time of flight (TOF) technique. An array of six Faraday cups positioned at 0, 15, 30, 45, 60 and 75° with respect to the anode axis, has been used. Due to the semi-hemispherical shape of the plasma plume after the pinch, the Faraday cups were located at different angular positions on a quadrant holder, all with the same radius distance with respect to the anode tip. The experiments were conducted under the assumption that the ion beam is azimuthally uniform. Furthermore, the plasma focus device was used as an apparatus for thin film deposition where targets were located on the anode tip. After the pinch, working gas ions move upward from the anode tip and the relativistic electrons bombard the target surface and create the second wave of ions. In the present study the angular distribution of secondary ions energy and flux has also been evaluated.

The outline of the manuscript is as follows: The description of experimental apparatus is given in section 2. The obtained data, the calculation methods, and the resultant curves along with related discussions are presented in section 3. Conclusions are drawn in section 4.

2. Experimental set-up

2.1. Plasma focus device

The experiments were conducted on a Mather-type plasma focus device comprising a 11 μF capacitor bank with maximum voltage of 30 kV (5 kJ energy). The plasma producing electrodes consisted of one 13.6 cm long OFHC copper rod as anode located at the center surrounded by six 12 cm long copper cathodes placed in a squirrel cage arrangement with an annular distance of 2 cm. The diameter of the anode rod was 2 cm and those of six cathode rods were 0.9 cm. A Pyrex insulator sleeve with 2 cm length and 0.25 cm thickness surrounded the bottom end of the anode separating the electrodes. The entire anode-cathode assembly was placed in a stainless-steel chamber. A rotary mechanical vacuum pump was employed to evacuate the chamber up to $4\times\ 10^{-2}$ mbar before the introduction of the filling gas. The experiments were performed with argon as filling gas, at the optimum operating pressure of 0.3 mbar and the charging voltage of 15 kV in all experiments. At these conditions, the peak current (current at pinch time) was 120 kA. The total circuit inductance was 140 nH and the quarter period was 2 μs.

2.2. Faraday cup

The Faraday cup is a charged particle detector, composed of two deep cylindrical electrically conductive electrodes separated by a dielectric. The inner collector detects the charged particles and the outer electrode which is grounded shields it from improper electromagnetic radiations. The charged particles enter the inner collector through a small aperture in order to confine the load. When charged particles impinge on the inner collector, a potential difference is generated between the two cylinders and passes through RG58, 50 Ω coaxial cable to the oscilloscope. The related circuit is showed in Fig. 1. The dimensions of the coaxial cylinders of Faraday cup must also be such that the impedance Z given by:

$$Z=\frac{138.2}{\sqrt{K}}\log_{10}\left(\frac{D}{d}\right) \tag{1}$$

is 50 Ω. Here D is the inside diameter of the outer electrode, d the outside diameter of the inner electrode and K is the dielectric constant. The Faraday cup signal recorded by oscilloscope is a voltage-time curve. With the assumption that the ions leave the pinch region at the same time, the X-ray peak which occurs as the pinch collapses and the ions fly upward, is considered as the origin of time for ions flight. It is also considered that the pinch region is negligible compared to the distance between the Faraday cup and the pinch region on top of the anode. Therefore, it is assumed that the flight distance is the same for all ions.

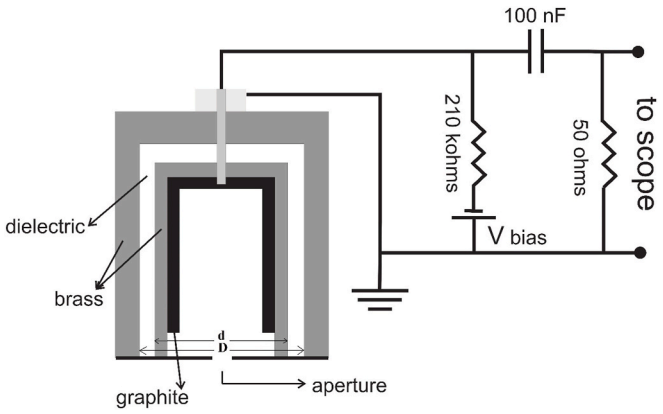

Fig. 1. Schematic diagram of the Faraday cup and related circuit.

Using ions time of flight, the corresponding velocity and non-relativistic energy is calculated by the simple relation:

$$E=\frac{1}{2}Mv^2 \tag{2}$$

Thus, the time axis in Faraday cup signal is related to the energy. The ions flux corresponding to each energy is calculated by

$$flux\left(\frac{ions}{m^2 s}\right)=\frac{V_{osc}}{RqA} \tag{3}$$

where V_{osc} is the voltage of the Faraday cup signal, R the resistance across the oscilloscope input signal (50 Ω), q the ions charge and A the area of the aperture. Therefore, the ion flux curve as a function of ion energy can be obtained.

The ion energy spectrum was measured by a Faraday cup assembly and TOF analysis. The schematic diagram of the PF device and the Faraday cup assembly is shown in Fig. 2. In order to have assessment of the ions' spectrum due to the plasma plume umbrella shape after the pinch, six identical Faraday cups placed on a quadrant holder were used simultaneously. All Faraday cups have the same radial distance of 7 cm from the anode tip. They are located at the angular positions 0, 15, 30, 45, 60 and 75° with respect to the anode axis. The Faraday cups are composed of two coaxial cylinders made up of brass and a dielectric between them. The dielectric was a sheet of PTFE Teflon with a dielectric constant of 2.1. The height of the Faraday cups was 20 mm with the inner diameter of the outer cylinder (D) and the outer diameter of the inner cylinder (d) 15 mm and 5 mm, respectively (Fig. 1). These dimensions are selected to avoid the impedance mismatch between Faraday cups and the 50 Ω transmission cable. The outer brass electrode plays the role of the grounded shield. In order to minimize the secondary electron emission, a graphite tube, which is used as the ion collector electrode, is inserted inside the inner brass cylinder. Graphite has shown to generate significantly a smaller number of secondary electrons emitted per incident ion [11]. Furthermore, the diameter to length ratio of the graphite collector (3 mm–15 mm) was in the range that minimizes the escape factor of the secondary electrons [12]. To reduce the signal to noise ratio, the Faraday cups outer brass electrode and the copper shields on the transmission cables were grounded. The Faraday cups were biased at −150 V throughout the experiments. In order to attenuate the ion signal, a plate with a 500 μm aperture was screwed to the bottom end of the Faraday cups. The ion signals of the six Faraday cups were recorded simultaneously by two four channel oscilloscopes.

As mentioned earlier, the aim of present work is to study the energy and flux of ions in PF device when it is used for thin film deposition or ion implantation. Besides the energy and flux of argon filling gas ion beams, energy and flux of target ions were also taken into account. When PF device is used for thin film deposition, the intended material for deposition is fixed on the anode tip. A set of three experiments was

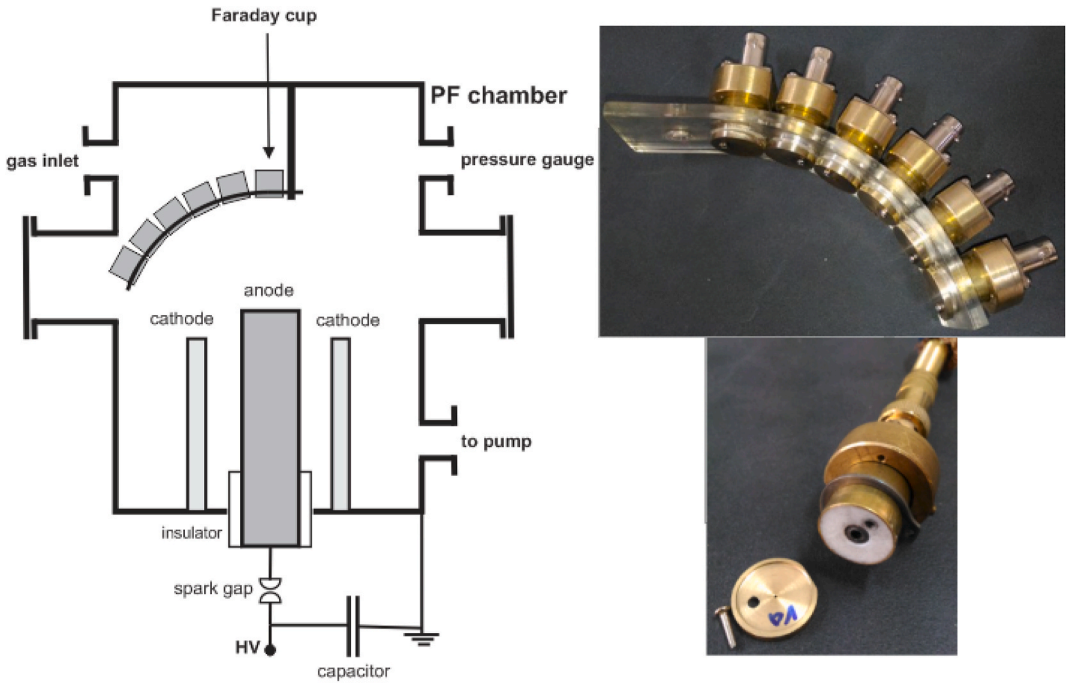

Fig. 2. Schematic diagram of PF device and Faraday cups assembly and configuration.

conducted with argon as the chamber filling gas along with three different targets of copper, graphite and tungsten. In each experiment, disc shaped target was screwed down on top of the anode, making the anode flat end. The results of the experiments are presented in the following section.

3. Results and discussion

The ion beams generated in the PF device were monitored by an assembly of six identical Faraday cups located at different angular positions at the same radial distance of 7 cm from the anode tip. Typical signals of Faraday cups located at the angular positions 0, 15, 30, 45, 60 and 75° with respect to the anode axis for different targets of copper, graphite and tungsten along with voltage probe signal are shown in Fig. 3. In order to have a proper interpretation of the signals registered by Faraday cups, a brief glance at successive PF device phases is helpful. In the PF devices, the application of a high voltage pulse between the electrodes initiates the breakdown phase. The filling gas as a result of dielectric breakdown forms a plasma layer (current sheath) through which the discharge current flows. The plasma generation process starts with the acceleration of free electrons which leads to ionization of the filling gas. The current sheath forms on the insulator surface or radially bridges the electrodes at the end of the insulator [13]. This initial phase ends up when the current sheath starts to move toward the electrodes open end by the Lorentz force. In this axial run-down phase, the current sheath accelerating along the electrodes creates a shock wave in front of it [14]. The gas that is swept up by the moving shock front is ionized and converts into plasma by the current flow [15]. When the current sheath reaches the open end of the electrodes, radial compression of the plasma occurs. The current sheath pushed by the inward Lorentz force, forms a dense hot plasma column and the plasma pinching process starts. At the final stage of the radial compression near the z-axis of the PF chamber, a cumulative plasma stream is produced on top of the anode which accelerates in the direction of z-axis with the energy of the order of keV. This axial cumulative plasma jet forms a shock wave above the anode. The hemispherical shock wave propagates along the z-axis through the medium [16–18]. A short period of time after the mentioned processes, a plasma diode is formed in the pinched plasma near the anode (proven by both experimental and theoretical studies [17,19,20]). Within this diode, at first fast electrons are accelerated towards the anode generating X-rays and then beams of fast ions with the energy of the order of 0.1–1 MeV move in the opposite direction. The fast ion beam takes little divergence before it reaches the hemispherical shock wave front [16]. Then it penetrates through the shock wave front into the medium and propagates with more divergence [17]. As is reported in literature, the height of the pinching area, namely from the anode top to the shock wave front, is different in various PF devices [18,21,22]. The Faraday cups distance from the anode determines which one of the fast ions or dense plasma stream first reaches the detectors [23]. If the Faraday cups are placed outside the pinching area (above the shock wave front), fast ions reach the Faraday cups first, since ions penetrate the shock wave front due to their MeV energy; afterwards, the dense plume of plasma streams, in their divergence movement, reach the Faraday cups. As mentioned earlier, in this study, Faraday cups are located at the same radial distance of 7 cm from the anode tip and ion signals registered by the array of Faraday cups are presented in Fig. 3. The common feature in all of Faraday cup signals for every target is the appearance of three main peaks. The first peak starting to shape once the pinch event ends, namely at the end of singularity in voltage probe signal, has been proven to be due to X-ray emission [24]. The emission of X-ray occurs as the electrons of the plasma diode collide with the anode surface at the end of pinching process. The signals of the Faraday cup located at 0°, for all three targets, show higher level of X-ray peak compared to previous reports [1–3]. This is due to the shape of the inserted anode targets in the present experiments, which made the anode flat end resulting in stronger collisions between electrons and the anode tip [25]. Furthermore, it is worth mentioning that as it is expected, a stronger X-ray peak is registered for tungsten target compared to copper and graphite targets (Fig. 4). In order to ascertain that the first peak is caused by X-ray emission, the ion entrance pinhole of the Faraday cups was covered by a plastic film with the thickness of <50 μm. The plastic film is transparent to X-rays and other strong electromagnetic radiations while it can obstruct flying ions to reach the Faraday cup collector. The typical signal of the entrance-covered Faraday cup along with the discharge current is shown in Fig. 5. The peak occurring simultaneously with the dip of the current signal, which is due to the pinch, is recorded and the second and

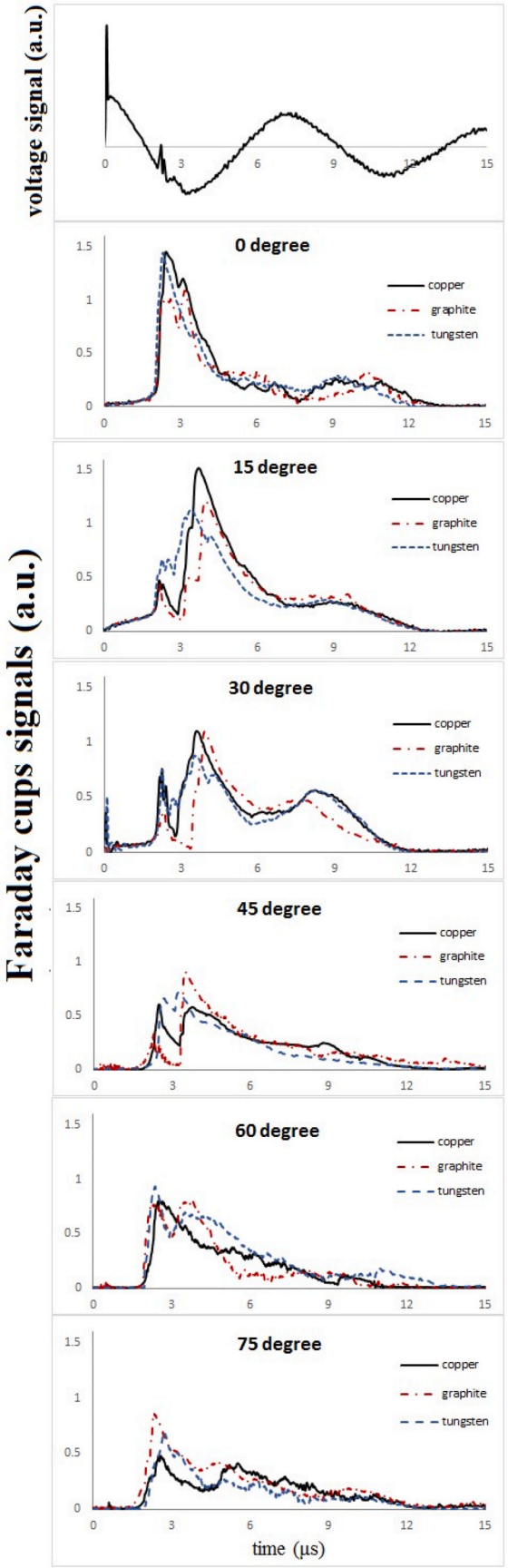

Fig. 3. Voltage probe and Faraday cup signals for copper, graphite and tungsten targets.

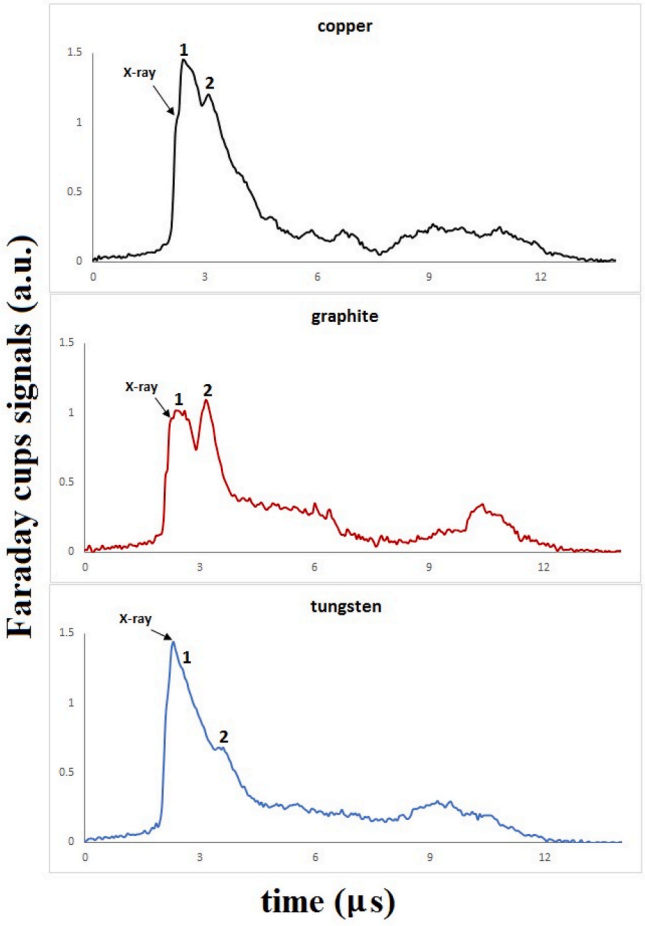

Fig. 4. 0° Faraday cup signals for targets of copper, graphite and tungsten. The first peak belongs to X-ray and peaks "1" and "2" belong to fast ion beams and plasma streams, respectively.

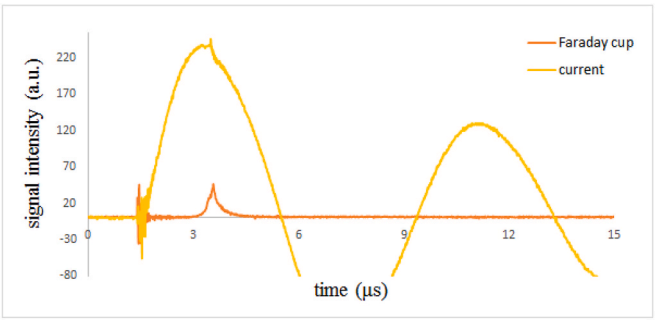

Fig. 5. Faraday cup signal when the pinhole entrance is covered by plastic film.

third peaks are vanished. It could be inferred that the first peak is not related to ions and it is totally due to the X-ray emission.

The second main peak is the strongest peak in almost all Faraday cup signals. However, there is slight change between the second main peak of the Faraday cup positioned at 0° with the other five Faraday cups signals. The dense plume of plasma streams is created prior to the X-ray, whereas there is no signal registered by the Faraday cups before the X-ray peak. Therefore, it can be inferred that the array of Faraday cups is located outside the pinching area. In this regard, it is expected that fast ion beams reach the Faraday cups first and soon after that plasma streams are registered. This is visible in the signal of 0° angular position Faraday cup, where the second main peak is actually composed of two

tightly adjacent sub-peaks. The primary sub-peak (peak1) is related to the fast ion beams and the secondary one (peak 2) belongs to plasma streams. To have an accurate sight, the signals of 0° Faraday cups of three targets are presented in Fig. 4 with slight magnification. Since fast ion beams diverge in a narrow solid angle, this peak is absent in the signals registered by the other five Faraday cups located off-axis (Fig. 3). As fast ion beams are created due to plasma diode and the result of pinching process, it would be expected that primary sub-peak (peak 1) does not show up in the signals pertaining to the shots with no pinch. In Fig. 6, two different signals are compared and it is apparent that the Faraday cup signal related to the no-pinch experiment has no primary sub-peak belonging to the fast ion beams. Comparison of the two signals proves that the primary sub-peak (peak 1) pertains to the fast ion beams.

The third main peak relates to the ions of target placed on the anode tip. When energetic electrons of the hot plasma collide with the target surface at the end of the pinching process, the ablated ions from the target surface splash upward. The magnitude of the third peak in the Faraday cup traces of the present study is much more substantial than what has been previously reported in literature [1–3]. This is due to the fact that targets screwed on top of the anode make it flat end rather than being hollow, hence more ions are ablated due to electrons collision. In order to verify that the third peak is indeed linked to the target ion beams, a typical Faraday cup signal obtained from a hollow anode was examined (Fig. 7). The inspection indicates that the third peak is nearly absent in the signals obtained from hollow anode. This confirms that the third peak belongs to target ions.

Energy spectra of both gas and target ions have been evaluated by TOF technique. The end of plasma pinch which coincides with the rise of X-ray pulse, has been taken as reference time for the onset of both gas and target ions flight. Typical *dN/dE* spectra of argon fast ion beams (peak 1) using the signal obtained from the Faraday cup placed at 0° angular position are shown in Fig. 8. As mentioned earlier fast ion beam signals occurred only at 0° Faraday cup. The maximum energy of

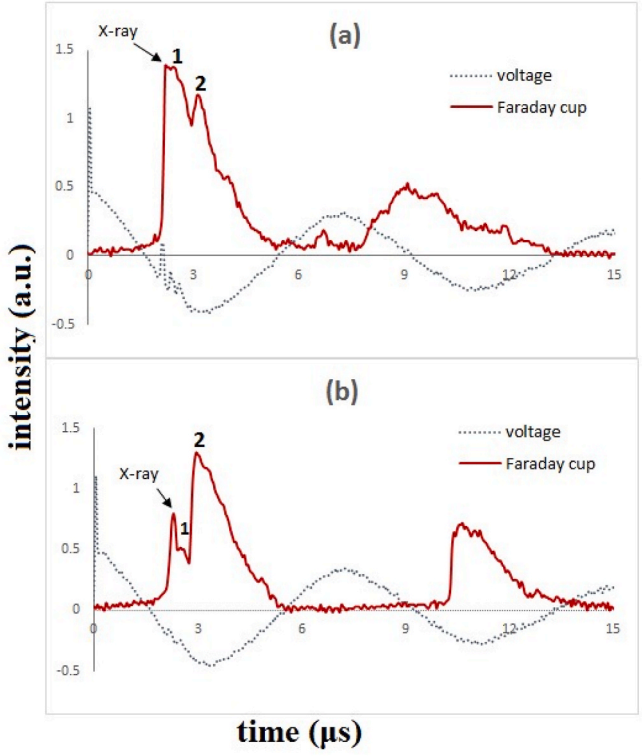

Fig. 6. Typical signals registered by 0° angular position Faraday cup with copper target. The experiment is carried out in a situation producing (a) strong pinch, and (b) almost no pinch, in which X-ray is weaker and peak "1" is nearly absent.

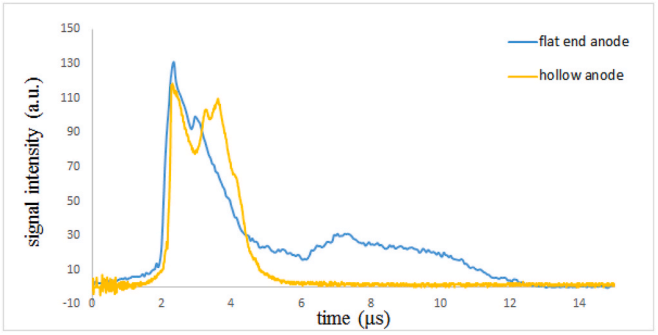

Fig. 7. Faraday cup signal when the experiment is performed by hollow anode.

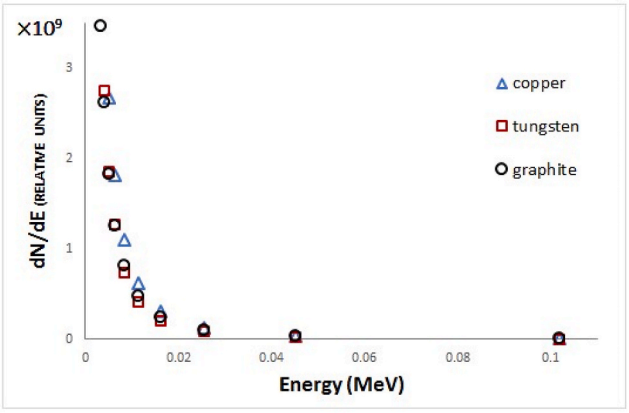

Fig. 8. Argon fast ion beams energy spectrum measured by data obtained from 0° Faraday cup for three different targets. Maximum fast ions energy for all targets are of the order of 0.1 MeV. Corrections were made for equilibrium charge state.

fast ions for all three targets are of the order of 0.1 MeV. The equation governing the behavior of *dN/dE* spectrum is given by Ref. [12]:

$$\frac{dN}{dE} = \left(\frac{Lm^{1/2}}{(2E)^{3/2}}\right)\left(\frac{V_{osc}}{eR(k\sigma + Z(E))}\right) \tag{4}$$

where L is the distance between Faraday cup and anode tip, m the mass of argon ions, σ the secondary electron emission for graphite collector [26], k the escape factor for the secondary electrons which is determined according to the Faraday cups dimensions [12]. The parameter $Z(E)$ is called the equilibrium charge state and is the changed charge of ions. It is used as a correction factor because beam ions capture and lose electrons to the chamber gas during the passage from focus to the Faraday cup entrance hole. This parameter is given by following equation [27]:

$$Z(E) = Z_p \frac{376x + x^6}{1428 - 1206x^{0.5} + 690x + x^6} \tag{5}$$

where Z_p is the projectile (argon ions) nuclear charge, and x is:

$$x = \left(\frac{v_p}{v_0} Z_p^{-0.52} Z_t^{0.03 - 0.017 Z_p^{-0.52} v_p / v_0}\right)^{1 + 0.4/Z_p} \tag{6}$$

Here v_0 is Bohr velocity (2.19×10^6 m/s), v_p is the projectile velocity and Z_t is the target nuclear charge. In this study the correction has not been made for energy attenuation and lateral spreading.

The registered ion signals have also been used to calculate the ion flux by averaging over a few similar shots. The results of ion flux as a function of ion energy are presented in Figs. 9 and 11. Fig. 9 shows the energy spectrum of argon plasma streams (argon ions which were mentioned as peak 2). Argon ions showed almost the same spectrum

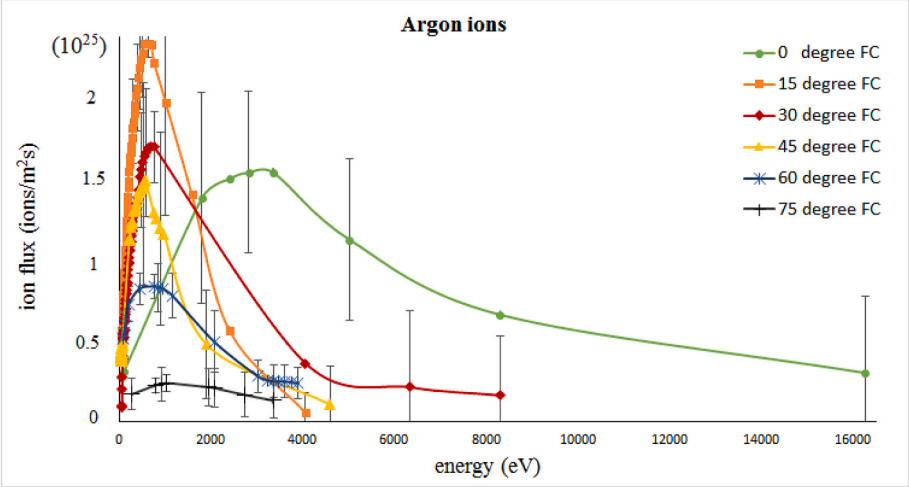

Fig. 9. Argon ions energy spectrum registered by Faraday cups located at 0, 15, 30, 45, 60- and 75-degrees angular positions with respect to anode.

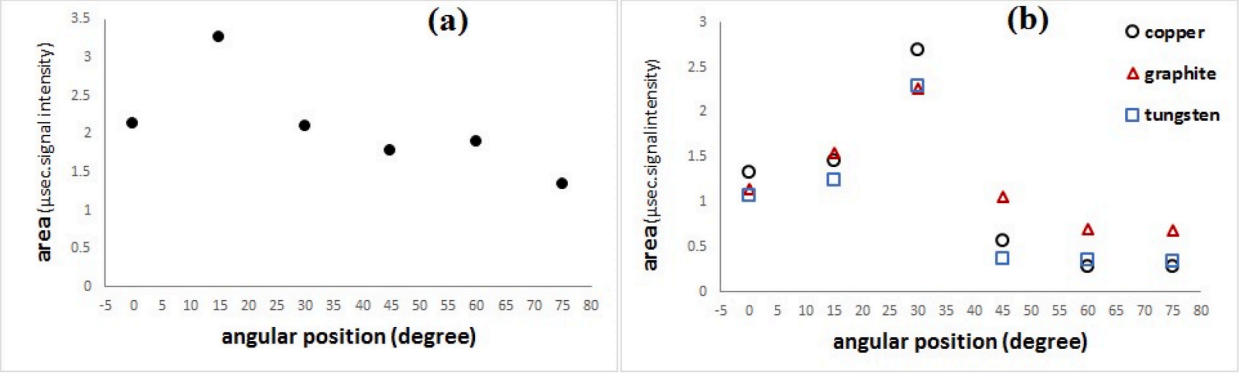

Fig. 10. The area under the curve of ion signals registered by Faraday cups located at different angular positions. (a) argon plasma ions and (b) target ions.

irrespective of the target material, hence the argon ion streams of copper target experiment have been considered as a typical case. As was expected, Faraday cups have registered a wide range of ions energy from a few keV to energies as low as tens of eV. The maximum energy of argon ions was recorded by the Faraday cup positioned at 0°; however, the highest flux was detected by the Faraday cup at 15°. This can be observed in Fig. 10(a) where the area under the curve of ion signals registered by oscilloscope (Fig. 3) are presented. It is evident from Fig. 9 that the ions flying towards the Faraday cup located at 0° expand over a wider energy range compared to the 15° Faraday cup. In this regard the energy spectrum curve of the 0° Faraday cup (Fig. 9) appears more extended. However, as was mentioned earlier, the overall ion flux calculated from the ions signal gathered by the oscilloscope shows that the area under the curve for the Faraday cup located at 15° is more stretched compared to 0° Faraday cup. It should be noted that in previous studies of chamber gas ion flux distribution in other PF devices, the data registered by polycarbonate track detectors [28,29] and CR-39 nuclear track detectors [30–32] also confirm that the maximum gas ion flux occurs at some degrees off the anode axis. The most probable energy recorded by Faraday cups at 0, 15, 30 and 45° were 3 keV, 710, 770 and 600eV, respectively. Although the ions moving right upward have higher energies, their numbers are less compared to those accelerating toward 15-degrees direction. The ions flux carrying most probable energy was 1.55×10^{25} ions/m^{2}s at 0°, while 2.35×10^{25} and 1.70×10^{25} ions/m^{2}s were recorded for 15 and 30°, respectively. The Faraday cups at 60 and 75° recorded the least value for ions energy and flux. These findings are consistent with those previously reported [30,33,34] that most ions in a cylindrical gas chamber accelerate towards mid-off axis directions.

The flux as a function of energy for target ions is presented in Fig. 11. An obvious anisotropy is also observed in both energy and flux of target ions for all three targets of copper, graphite and tungsten. The area under the curve of target ion signals is presented in Fig. 10(b). The common feature is that the highest flux for target ions occurs at 30° angular position irrespective of the target material. However, Fig. 11 shows that the angular position at which the highest value of most probable energy occurs, depends on the target material. The highest value of most probable energy maximizes at 0° angular position in the case of argon-tungsten experiment, while for copper and graphite targets it occurs at 30° angular position. Similar to argon ions, target ions move towards 45, 60- and 75-degrees directions with least energy and flux irrespective of the target material. It is interesting to note that for thin film deposition in PF device, angular positions consisting of target ions with higher energy, resulted in more irregular surfaces. In a previous report concerning tungsten deposition by PF device, samples located at 0° showed more irregular surface compared to those at 30° [10]. In yet another experiment for deposition of graphite, samples located at 30° experienced rough surface deposition compared to 0° angular substrate location [9]. Regular surfaces along with crystal structures and interatomic bonds have been observed for substrates located at 60 and 75° receiving less energetic target ions [9]. As far as deposition process is concerned, more energetic gas and target ions moving toward near axis angular positions result in different properties compared to those flying far off axis. This is due to the significant difference in energy and flux of ions at various angular positions. Furthermore, these findings imply that for ion implantation processes in which high energetic ions are needed,

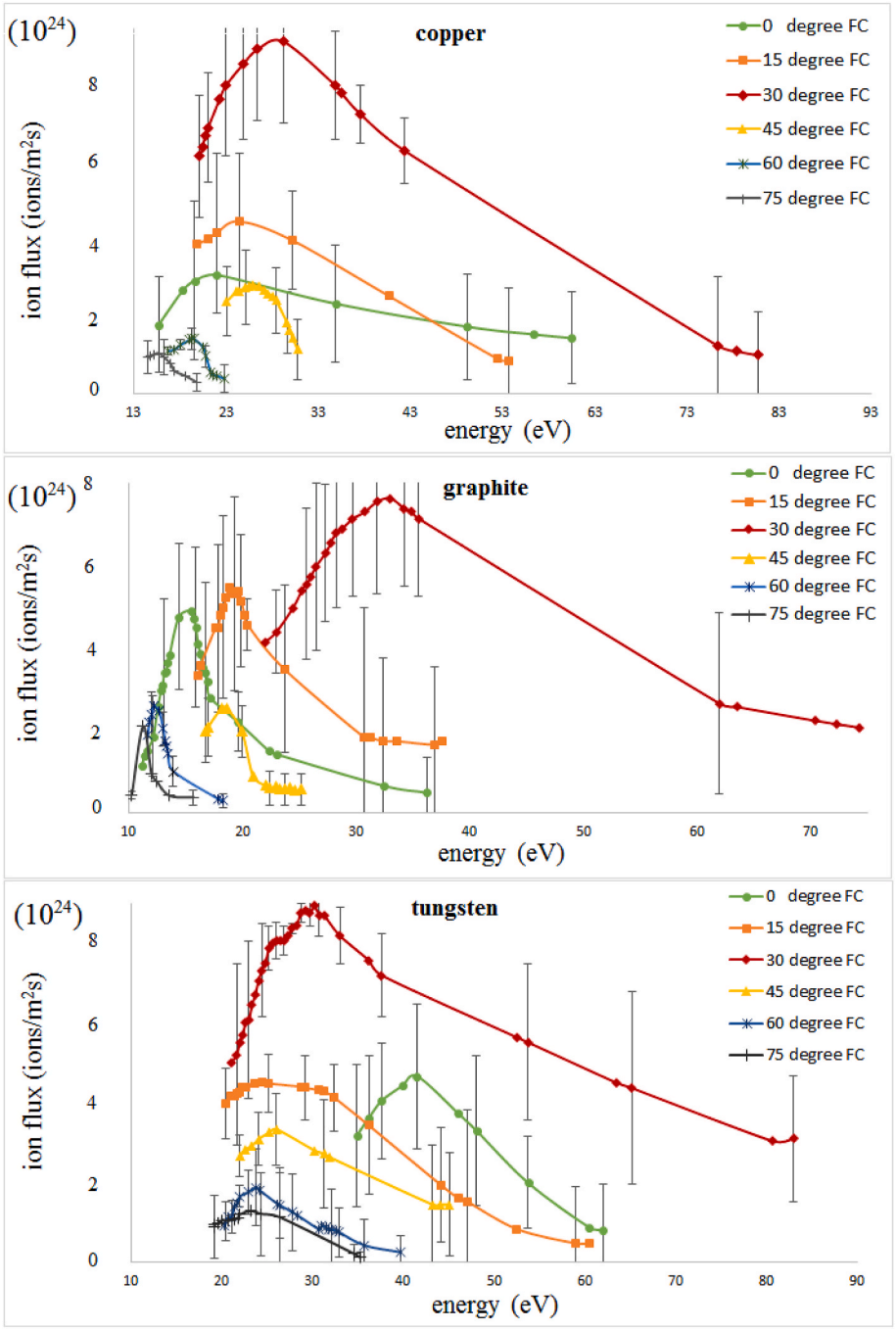

Fig. 11. Ion energy spectrum relating to three different targets of copper, graphite and tungsten.

on axis positions are more proper if gas ions are intended to be implanted and 30° angular position are more apt if target ions are to be implanted except for tungsten targets where 0° is more suitable for ion implantation.

4. Conclusion

The temporal and spatial distribution of argon gas and three different target ions in a plasma focus device was investigated by an assembly of six identical Faraday cups placed at different angular positions. The Faraday cups signals depicted three main peaks. The first peak occurring simultaneously with the pinch event on the voltage probe signal, was proved to be X-ray signal. The second main peak which was the highest and the temporally longest one, attributed to argon gas ions. In the second main peak, the primary sub-peak was related to fast ion beams which were the product of plasma diode as the final stage of pinching process and the secondary sub-peak was related to the cumulative plasma streams which were produced during radial compression. The complementary experiments confirmed that the third peak is relevant to the target ions. Plots of ion flux as a function of ions energy for argon plasma streams indicates that ions traveling towards 0° direction, had the highest most probable energy. However, the largest ion flux was recorded by the Faraday cup located at 15°. Considering target ions, the common fact observed in three different targets of copper, graphite and tungsten was that the largest flux took place at 30° angular position. However, the most probable energy had the highest value at 0° angular position for tungsten target and at 30° angular position for copper and graphite targets.

Data availability

The data that support the findings of this study are available from the corresponding author upon reasonable request.

Declaration of competing interest

The authors declare that they have no known competing financial interests or personal relationships that could have appeared to influence the work reported in this paper.

References

[1] M. Bhuyan, N.K. Neog, S.R. Mohanty, C.V.S. Rao, P.M. Raole, Temporal and spatial study of neon ion emission from a plasma focus device, Phys. Plasmas 18 (3) (2011), 033101.

[2] H. Bhuyan, M. Favre, E. Valderrama, H. Chuaqui, E. Wyndham, Experimental studies of ion beam anisotropy in a low energy plasma focus operating with methane, J. Phys. Appl. Phys. 39 (16) (2006) 3596.

[3] S.R. Mohanty, H. Bhuyan, N.K. Neog, R.K. Rout, E. Hotta, Development of multi Faraday cup assembly for ion beam measurements from a low energy plasma focus device, Jpn. J. Appl. Phys. 44 (7R) (2005) 5199.

[4] M. Sadowski, E. Rydygier, H. Herold, U. Jäger, H. Schmidt, Multi-spike structure of ion pulses generated by plasma focus discharges, Phys. Lett. 113 (1) (1985) 25–31.

[5] M. Sadowski, E. Skladnik-Sadowska, J. Baranowski, J. Zebrowski, H. Kelly, A. Lepone, A. Marquez, M. Milanese, R. Moroso, J. Pouzo, Comparison of characteristics of pulsed ion beams emitted from different small PF devices, Nukleonika 45 (3) (2000) 179–184.

[6] H.R. Yousefi, Y. Nakata, H. Ito, K. Masugata, Characteristic observation of the ion beams in the plasma focus device, Plasma Fusion Res. 2 (2007). S1084-S1084.

[7] R. Antanasijević, Z. Marić, J. Vuković, B. Grabež, D. Djordjević, D. Joksimović, V. Udovičić, A. Dragić, J. Stanojević, R. Banjanac, D. Joković, Angular distribution of protons emitted from the hydrogen plasma focus, Radiat. Meas. 36 (1–6) (2003) 327–328.

[8] A. Szydlowski, A. Banaszak, B. Bienkowska, I.M. Ivanova-Stanik, M. Scholz, M. J. Sadowski, Measurements of fast ions and neutrons emitted from PF-1000 plasma focus device, Vacuum 76 (2–3) (2004) 357–360.

[9] F.M. Aghamir, A.R. Momen-Baghdadabad, M. Etminan, Effects of deposition angle on synthesis of amorphous carbon nitride thin films prepared by plasma focus device, Appl. Surf. Sci. 463 (2019) 141–149.

[10] F.M. Aghamir, A.R. Momen-Baghdadabad, Characteristics of tungsten layer deposited on graphite substrate by a low energy plasma focus device at different angular position, Thin Solid Films 685 (2019) 108–116.

[11] G.R. Etaati, R. Amrollahi, M. Habibi, R. Baghdadi, Angular distribution of argon ions and X-ray emissions in the APF plasma focus device, J. Fusion Energy 30 (2) (2011) 121–125.

[12] M. Mohammadnejad, S.J. Pestehe, M.A. Mohammadi, Energy spectrum of argon ions emitted from Filippov type Sahand plasma focus, Rev. Sci. Instrum. 84 (7) (2013), 073505.

[13] H. Bruzzone, R. Vieytes, The initial phase in plasma focus devices, Plasma Phys. Contr. Fusion 35 (12) (1993) 1745.

[14] Marek Rabiński, Krzysztof Zdunek, Physical model of dynamic phenomena in impulse plasma coaxial accelerator, Vacuum 48 (7–9) (1997) 715–718.

[15] M.G. Haines, Dense plasma in Z-pinches and the plasma focus, Phil. Trans. Roy. Soc. Lond. Math. Phys. Sci. 300 (1456) (1981) 649–663.

[16] Valeriy N. Pimenov, Elena V. Demina, L.I. Ivanov, V.A. Gribkov, A.V. Dubrovsky, U. Ugaste, T. Laas, et al., Damage and modification of materials produced by pulsed ion and plasma streams in Dense Plasma Focus device, Nukleonika 53 (2008) 111–121.

[17] V.A. Gribkov, C. Tuniz, E.V. Demina, A.V. Dubrovsky, V.N. Pimenov, S. V. Maslyaev, R. Gaffka, et al., Experimental studies of radiation resistance of boron nitride, C2C ceramics Al2O3 and carbon–fiber composites using a PF-1000 plasma-focus device, Phys. Scripta 83 (4) (2011), 045606.

[18] V.A. Gribkov, Physical processes taking place in dense plasma focus devices at the interaction of hot plasma and fast ion streams with materials under test, Plasma Phys. Contr. Fusion 57 (6) (2015), 065010.

[19] S. Lee, S.H. Saw, Plasma focus ion beam fluence and flux—scaling with stored energy, Phys. Plasmas 19 (11) (2012) 112703.

[20] V.A. Gribkov, A. Banaszak, B. Bienkowska, A.V. Dubrovsky, I. Ivanova-Stanik, L. Jakubowski, L. Karpinski, et al., Plasma dynamics in the PF-1000 device under full-scale energy storage: II. Fast electron and ion characteristics versus neutron emission parameters and gun optimization perspectives, J. Phys. Appl. Phys. 40 (12) (2007) 3592.

[21] Leopoldo Soto, Cristian Pavez, José Moreno, Mario Barbaglia, Alejandro Clausse, Nanofocus: an ultra-miniature dense pinch plasma focus device with submillimetric anode operating at 0.1 J, Plasma Sources Sci. Technol. 18 (1) (2008), 015007.

[22] José Moreno, Patricio Silva, Leopoldo Soto, Optical observations of the plasma motion in a fast plasma focus operating at 50 J, Plasma Sources Sci. Technol. 12 (1) (2002) 39.

[23] V.A. Gribkov, Ye S. Grebenschikova, Ye V. Demina, A.V. Dubrovsky, A.V. Kovtun, O.N. Makeev, K. Malinowski, et al., Damages of carbon-tungsten samples under influence of deuterium ions and dense plasma streams within plasma-focus facility, in: AIP Conference Proceedings vol. 993, American Institute of Physics, 2008, pp. 361–364, 1.

[24] H. Kelly, A. Lepone, A. Marquez, M.J. Sadowski, J. Baranowski, E. Skladnik-Sadowska, Analysis of the nitrogen ion beam generated in a low-energy plasma focus device by a Faraday cup operating in the secondary electron emission mode, IEEE Trans. Plasma Sci. 26 (1) (1998) 113–117.

[25] M. Zakaullah, Imtiaz Ahmad, A. Omar, G. Murtaza, M.M. Beg, Effects of anode shape on plasma focus operation with argon, Plasma Sources Sci. Technol. 5 (3) (1996) 544.

[26] J.M. Pedgley, G.M. McCracken, H. Farhang, B.H. Blott, Measurements of secondary electron emission for fusion related materials, J. Nucl. Mater. 196 (1992) 1053–1058.

[27] G. Schiwietz, P.L. Grande, Improved charge-state formulas, Nucl. Instrum. Methods Phys. Res. Sect. B Beam Interact. Mater. Atoms 175 (2001) 125–131.

[28] M. Sohrabi, M. Habibi, G.H. Roshani, V. Ramezani, A novel method for observation by unaided eyes of nitrogen ion tracks and angular distribution in a plasma focus device using 50 Hz–HV electrochemically-etched polycarbonate detectors, Radiat. Meas. 47 (7) (2012) 530–536.

[29] M. Sohrabi, M. Habibi, V. Ramezani, Helium ion distributions in a 4 kJ plasma focus device by 1 mm-thick large-size polycarbonate detectors, Phys. Lett. 378 (48) (2014) 3631–3637.

[30] M. Sadowski, J. Zebrowski, E. Rydygier, J. Kucinski, Ion emission from plasma-focus facilities, Plasma Phys. Contr. Fusion 30 (6) (1988) 763.

[31] Marek Sadowski, Elzbieta Skladnik-Sadowska, Jaroslaw Baranowski, Jaroslaw Zebrowski, Hector Kelly, Alejandro Lepone, Adrianna Marquez, Maria Milanese, Roberto Moroso, Jorge Pouzo, Comparison of characteristics of pulsed ion beams emitted from different small PF devices, Nukleonika 45 (3) (2000) 179–184.

[32] Mehdi Sohrabi, Breakthroughs in 4π panorama ionology in plasma focus devices for mechanisms understanding with special regards to hydrogen ions (protons), Radiat. Meas. 119 (2018) 192–198.

[33] J. Prokůpek, J. Kaufman, D. Margarone, M. Krůs, A. Velyhan, J. Krása, T. Burris-Mog, S. Busold, O. Deppert, T.E. Cowan, G. Korn, Development and first experimental tests of Faraday cup array, Rev. Sci. Instrum. 85 (1) (2014), 013302.

[34] Smruti Ranjan Mohanty, et al., Effect of anode designs on ion emission characteristics of a plasma focus device, Jpn. J. Appl. Phys. 46 (5R) (2007) 3039.